Available online at www.sciencedirect.com
SCIENCE DIRECT®
Journal of Nuclear Materials 352 (2006) 300–308
journal of nuclear materials
www.elsevier.com/locate/jnucmat

Modelling heat capacity, thermal expansion, and thermal conductivity of dioxide components of inert matrix fuel

V. Sobolev *, S. Lemehov

Belgian Nuclear Research Centre, SCK·CEN, Boeretang 200, B-2400 Mol, Belgium

Abstract

Based on a simplified model of the phonon spectrum, on the statistical thermodynamics, and on the generalised Klemens model for thermal conductivity, some useful relationships bounding the specific heat capacity, the thermal expansion coefficient, the bulk modulus and the thermal conductivity of dioxides, often used as components in inert matrix fuel, were deduced in a quasi-harmonic approximation. The developed models were first verified with urania UO_2, then applied for prediction of the isobaric specific heat, the isobaric thermal expansion coefficient, and the thermal conductivity of ThO_2 and of one inert matrix material: ZrO_2. The similarity principle was used in the cases where the input data were missing. The obtained results were compared with the available experimental data, and satisfactory agreement was demonstrated in the temperature range of 30–1600 K. In most of the cases the predicted values were within the region of the dispersion of the experimental data. The largest difference was observed for the thermal conductivity of ZrO_2 at high temperatures, which could be explained by unaccounted photon contribution.

PACS: 65.40.Ba; 65.40.De; 66.70.+f

1. Introduction

Modelling of thermal and mechanical properties of innovative fuels with matrices composed of low fissile or inert oxides is a problem of considerable importance in the design of new generation reactors. In the literature, these data are scarce and often show a wide spread because of the difficulties related to the measurement. Different sophisticated techniques have been used by different teams for the estimation of the thermomechanical properties of the actinide oxides and oxide matrices, e.g. [1–3]. These techniques, however, are difficult to implement in the fuel performance and design codes. On the other hand, simple empirical expressions often used in the engineering practice are not appropriate for prediction of new material properties and even can lead to completely erroneous data at large extrapolation. In many cases, a combined simplified physical modelling of a set of properties allow to deduce a missing property using the available data for similar materials.

In the present article, this approach is applied to two components of oxide IMF: ThO_2, and ZrO_2. The next chapter gives a brief reminder about the equation of state (EOS) and its use for calculation

* Corresponding author. Tel.: +32 14 33 22 67; fax: +32 14 32 15 29.
E-mail address: vsobolev@sckcen.be (V. Sobolev).

0022-3115/$ - see front matter © 2006 Elsevier B.V. All rights reserved.
doi:10.1016/j.jnucmat.2006.02.077

of the thermophysical properties of solids. A simplified model of the phonon spectrum used in EOS is proposed in the third section. In the fourth section, the relationships for the specific heat, the bulk modulus, and the coefficient of thermal expansion (CTE) of the considered oxide systems are deduced, aiming at their possible implementation into fuel performance codes. The formula for thermal conductivity based on these results and on the approach of Klemens is presented in the fifth chapter. At the end, the results of the model validation with UO_2 data and its application for prediction of the isobaric specific heat, the isobaric thermal expansion coefficient and the thermal conductivity of ThO_2 and of one inert matrix material – ZrO_2 – are presented and compared with the experimental data found in the literature.

2. Equation of state and relations between thermal and mechanical properties

The equation of state (EOS) is a key function for the determination of the properties of solids. The Helmholtz free energy $F = F(V,T)$, presented as a function of volume (V) and temperature (T), is often used as a caloric EOS. The main thermodynamic (TD) parameters – the isothermal bulk modulus (B_T), the isobaric volumetric CTE (α_p), the isochoric and isobaric heat capacities (C_V and C_p) – can be deduced from free energy F as follows [4]:

$$B_T(T,V) \equiv -V \cdot \left(\frac{\partial p}{\partial V}\right)_T = V \cdot \left(\frac{\partial^2 F}{\partial V^2}\right)_T, \tag{1}$$

$$\alpha_p(T,V) \equiv \frac{1}{V}\left(\frac{\partial V}{\partial T}\right)_p = -\frac{1}{B_T(V,T)} \cdot \left(\frac{\partial}{\partial T}\left(\frac{\partial F}{\partial V}\right)_T\right)_V, \tag{2}$$

$$C_V(T,V) \equiv \left(\frac{\partial U}{\partial T}\right)_V = -T\left(\frac{\partial^2 F}{\partial T^2}\right)_V, \tag{3}$$

$$C_p(T,V) = C_V(T,V) + \alpha_p^2(T,V) \cdot B_T(T,V) \cdot V \cdot T. \tag{4}$$

The microscopic statistical approach, used for the EOS deduction, considers a solid as a 'special box' filled with a gas of quasi-particles representing atom vibrations (phonons) and electronic excitations. The Helmholtz free energy of this system is a sum of the solid energy at $T = 0K(E_0)$, the contributions of phonons (F_{ph}), and the electronic excitations (F_{el}):

$$F(V,T) = E_0(V) + F_{ph}(V,T) + F_{el}(V,T). \tag{5}$$

In the quasi-harmonic approximation, the temperature dependent part of the phonon free energy of the ideal solid is [5]:

$$F_{ph}(V,T) = 3N_{at} \cdot k_B \cdot T \cdot \sum_i \int_{\omega_{0i}}^{\omega_{\max i}} \ln\left(1 - e^{-\frac{\hbar\cdot\omega(V)}{k_B T}}\right) \cdot f_i(\omega(V)) \cdot d\omega, \tag{6}$$

where k_B and $\hbar$ are the Boltzmann and Planck constants, respectively; N_{at} – number of atoms in the volume V; ω – phonon angular frequency; $f(\omega)$-phonon density-of-states function (DOS); i is the index of the phonon branch.

In the range of temperatures of interest ($T < 1600$ K), the temperature dependent part of the electronic component of the Helmholtz potential (F_{el}) for the oxides of interest can either be neglected, or determined by the excitations of the unpaired localised electrons [6]:

$$F_{el}(V,T) = -k_B \cdot T \cdot \ln \sum_j g_j \cdot \exp\left(\frac{-E_{ej}(V)}{k_B \cdot T}\right), \tag{7}$$

where E_{ej} – electron excitation energy at the jth level; g_j – degeneracy of the jth level.

In order to construct the EOS described by Eq. (5)–(7), the spectra of phonons and electronic excitations for the considered solids have to be known.

3. Dispersion function and phonon spectrum

The phonon spectrum of any isotropic solid consists of three acoustic translational vibration branches (one with the longitudinal polarisation – LA, and two with the transverse polarisation – TA_1 and TA_2) and $3N_{cell} - 3$ internal optical branches (where N_{cell} is the number of atoms in the primitive crystal cell). Taking into account the difficulties in determination of the phonon spectrum and complexity of the spectrum itself, simplified models are usually used in practice to estimate material properties. The application of the most known Debye model is limited to solids with one atom in the primitive cell when optic modes are absent. A simple possibility to take into account the optical phonons is to describe them with the Einstein model where the vibrations of all atoms have the same frequency. However, in many cases it is far from the reality and can also lead to incorrect results for solids with complex unit cells where the optical phonons are distributed in a large frequency region.

In this work, we propose to use for the considered dioxides a model of the phonon spectrum

where each acoustic branch is represented by the Debye type DOS-function and the optic branches are condensed into one longitudinal and two transverse branches described by using the well-known stepwise function Sign(x). In this case, the normalised to unity phonon DOS-function can be presented in the following form:

$$f_{\mathrm{ph}}(\omega) = \frac{1}{3N_{\mathrm{cell}}} \cdot \left(\sum_{i=1}^{3} \frac{\omega^2 \cdot \mathrm{Sign}(\omega_{i\mathrm{A}} - \omega)}{\omega_{i\mathrm{A}}^3} + 3 \cdot (N_{\mathrm{cell}} - 1) \cdot \sum_{i=4}^{6} \frac{\mathrm{Sign}(\omega - \omega_{i\mathrm{O\,min}}) - \mathrm{Sign}(\omega - \omega_{i\mathrm{O\,max}})}{(\omega_{i\mathrm{O\,max}} - \omega_{i\mathrm{O\,min}})} \right). \quad (8)$$

The minimum frequency of the acoustic branches is zero; the maximum frequencies can be found from the dispersion relations: $\omega_{\mathrm{A}i} = k_{\max} \cdot u_i = \pi \cdot u_i / a'$, where u_i is the sound velocity (determined by the elastic constant); i – index of polarisation (longitudinal or transverse); $k_{\max} = \pi/a'$ is the maximum phonon wave-vector determined by the Bragg's limitation; a' – the distance between the centres of the neighbour primitive cells.

The maximum and minimum frequencies for the optic branches cannot be calculated in this model. They should be found separately. For some of the considered oxides these frequencies are well known (e.g. for UO_2 [7]), for others they can be estimated using the similarity principle or simplified lattice dynamics models.

The proposed model gives a more realistic description of the total phonon spectrum than one-frequency Debye model or the combined Debye–Einstein approach. It has already been applied to actinide dioxides and allowed to obtain rather good results in a wide temperature range [8].

4. Heat capacity and thermal expansion

On the basis of the phonon spectrum (8) and the energy levels of electron excitations, one can construct the components (6) and (7) of the EOS for the considered system and then deduce formulae for heat capacity and CTE from (2)–(4). The isochoric heat capacity can be expressed as follows:

The characteristic temperatures $\theta_i \equiv \hbar \cdot \omega_i / k_{\mathrm{B}}$ and $\theta_{\mathrm{e}j} \equiv E_{\mathrm{e}j}/k_{\mathrm{B}}$ were introduced in formula (9) in the place of the phonon minimum and maximum frequencies and of the electron excitation energies, respectively, and also the 2nd kind Debye integral normalised to unity:

$$D'_n(y) = n \cdot y^{-n} \cdot \int_0^y x^{n+1} \cdot \exp(x) \cdot (\exp(x) - 1)^{-2} \mathrm{d}x.$$

The thermal expansion of solids is determined by anharmonic interactions between their atoms. The lattice anharmonicity leads to the volume dependence of the phonon frequencies, which is explicitly described by the Grüneisen parameters of the phonon branches $\gamma_{\mathrm{G}i} \equiv -\partial(\ln\langle\omega_i(V)\rangle)/\partial(\ln V) = -\partial(\ln\theta_i(V))/\partial(\ln V)$. Assuming that the spectrum of electronic excitations is independent of temperature and that the Grüneisen parameters are constant and the same in all the modes (i.e. $\gamma_{\mathrm{G}i} = \gamma_{\mathrm{G}}$), one can obtain from (2) for the considered oxide systems the well-known relationship for the isobaric volumetric CTE [9]:

$$\alpha_p(V,T) = \frac{\gamma_{\mathrm{G}} \cdot C_V(V,T)}{B_T(T) \cdot V(T)}. \quad (10)$$

Then the isobaric heat capacity C_p can be calculated with Eq. (4) presented in the following form:

$$C_p(T,V) = C_V(T,V) \cdot \left(1 + \frac{\gamma_{\mathrm{G}}^2 \cdot T \cdot C_V^{(V,T)}}{B_T(T) \cdot V(T)} \right). \quad (11)$$

5. Thermal conductivity

It is well known that thermal conductivity in the oxides of interest is mostly determined by the phonon mechanism. Other mechanisms (charge carriers, photons, vacancies) give only few percent

$$C_V = \frac{k_{\mathrm{B}} \cdot N_{\mathrm{at}}}{N_{\mathrm{cell}}} \cdot \left[\sum_{i=1}^{3} D'_3(\theta_{i\max}/T) + 3 \cdot (N_{\mathrm{cell}} - 1) \sum_{i=4}^{6} \left(\frac{\theta_{i\max} \cdot D'_1(\theta_{i\max}/T) - \theta_{i\min} \cdot D'_1(\theta_{i\min}/T)}{\theta_{i\max} - \theta_{i\min}} \right) \right] + \frac{k_{\mathrm{B}} \cdot N_{\mathrm{at}}}{3} \cdot \sum_j g_j \cdot \left(\frac{\theta_{\mathrm{e}j}}{T} \right)^2 \cdot \frac{\exp(\theta_{\mathrm{e}j}/T)}{(\exp(\theta_{\mathrm{e}j}/T) - 1)^2}. \quad (9)$$

contribution at sufficiently high temperatures, therefore they will be disregarded in this article. The phonon contribution to thermal conductivity (κ) in solids can be described using the Callaway type expression based on kinetic theory and the free path length (l) approach [10]:

$$\kappa_{\mathrm{ph}}(T) = \frac{1}{3}\sum_i \int_{\omega_{i\min}}^{\omega_{i\max}} c_i(\omega)\cdot u_i(\omega)\cdot l_i(\omega)\cdot \mathrm{d}\omega, \tag{12}$$

where $c_i(\omega)$ is the heat capacity of the ith branch phonons with the frequencies from ω to $\omega+\mathrm{d}\omega$ containing in the unit volume of the given solid, $u_i(\omega)$ – the phonon group velocity, $l_i(\omega)$ the phonon free path length determined by interactions with static and dynamic defects.

Expression (12) can be presented in another form as a product of the lower classic limit of the thermal conductivity (κ_0) and a sum of the dimensionless transport integrals $I_i(\theta_i/T)$ of the phonons branches:

$$\begin{aligned}\kappa_{\mathrm{ph}}(T) &= (k_{\mathrm{B}}\cdot n_{\mathrm{at}}\cdot l_0\cdot u_0)\\ &\quad\cdot\sum_i^{3N_{\mathrm{cell}}}\int_0^{\theta_i/T}\frac{U_i(x)\cdot\Lambda_i(x)\cdot x^2\cdot \mathrm{e}^x\cdot f_i(x)\cdot \mathrm{d}x}{(\mathrm{e}^x-1)^2}\\ &= \kappa_0\cdot\sum_i^{3N_{\mathrm{cell}}} I_i(\theta_i/T),\end{aligned} \tag{13}$$

where n_{at} is the number of atoms per unit volume; l_0 is the minimum phonon path length determined by the Bragg's condition; u_0 – the mean sound velocity; $U_i(x)\equiv u_i(x)/u_0$ is the relative phonon velocity and $\Lambda_i(x)\equiv l_i(x)/l_0$ is the relative phonon path length.

The Debye spectrum and the thermal conductivity model based on formula (12) has already been used by the authors in [11] for the modelling of self-irradiation effects. In the present article, we neglect the contribution of N-processes (so limiting the modelling to defect materials), but use the advanced model of the phonon spectrum. The effect of defects on the phonon spectrum is still disregarded. In the considered model of the phonon spectrum (8) described above, the acoustic phonon velocities are constant and those of the optic phonons are zero. In this case, substitution of spectrum (8) into (13) allows obtaining:

$$\kappa_{\mathrm{ph}}(T) = \frac{\kappa_0}{3N_{\mathrm{cell}}}\cdot\left(\frac{u_{\mathrm{AL}}}{u_0}\cdot\left(\frac{T}{\theta_{\mathrm{AL}}}\right)^3\cdot\int_0^{\theta_{\mathrm{AL}}/T}\frac{\Lambda_{\mathrm{AL}}(x)\cdot x^4\cdot \mathrm{e}^x\cdot \mathrm{d}x}{(\mathrm{e}^x-1)^2}+\frac{2u_{\mathrm{AT}}}{u_0}\cdot\left(\frac{T}{\theta_{\mathrm{AT}}}\right)^3\cdot\int_0^{\theta_{\mathrm{AT}}/T}\frac{\Lambda_{\mathrm{AT}}(x)\cdot x^4\cdot \mathrm{e}^x\cdot \mathrm{d}x}{(\mathrm{e}^x-1)^2}\right). \tag{14}$$

At $\Lambda(x)=1$, the phonon path length is the smallest allowed, and the expression (13) yields the lowest limit of the thermal conductivity:

$$\kappa_{\mathrm{ph}}(T) = \frac{\kappa_0}{3N_{\mathrm{cell}}}\cdot\left(\frac{u_{\mathrm{AL}}}{u_0}\cdot D_3'(\theta_{\mathrm{AL}}/T)+\frac{2u_{\mathrm{AT}}}{u_0}\cdot D_3'(\theta_{\mathrm{AT}}/T)\right). \tag{15}$$

In order to evaluate correctly the lattice thermal conductivity, three type of interactions: the phonon–phonon interactions (N-processes and U-processes) and the phonon scattering by different static defects (D) should normally be considered [11,12]. Assuming their independence, the resulting inverse phonon free path length can be presented as a sum:

$$\Lambda_i^{-1}(\omega) = \sum_k \Lambda_{\mathrm{D}i}^{-1}(\omega) + \Lambda_{\mathrm{ph}}^{-1}(\omega). \tag{16}$$

Two types of static defects are of major importance in the considered systems: point defects and crystallite boundaries. The phonon free path length limited by the scattering on the crystallite boundaries can be described with the Casimir formula [13] through the effective crystallite size $d_{\mathrm{Db\,eff}}$:

$$\Lambda_{\mathrm{Db}} = d_{\mathrm{Db\,eff}}/l_0. \tag{17}$$

The phonon interactions with point defects are usually estimated with the formula obtained by Klemens [14], which can also be presented as follows:

$$\Lambda_{\mathrm{Dp}} = \frac{l_{\mathrm{Dp}(i)}(\omega)}{l_0} = A_{\mathrm{point}}\cdot\left(\frac{\omega_{i\max}}{\omega}\right)^4 \tag{18}$$

with the dimensionless constant A_{point} depending on the lattice constant, elastic and thermal properties [15]. It is essential for the Klemens formula that point defects are isolated, immobile and the size of a sphere associated with a defect is small compared to the phonon wavelength. In many real cases, however, considering high temperature thermal conductivity the first two conditions are not formally satisfied and therefore the point defects microscopic cross-sections are overestimated. The

effective characteristic size of crystallites ($d_{\mathrm{Db\,eff}}$) and the point defect coefficient (A_{point}) can be found with the help of the microscopic analysis of the studied samples or estimated from the low temperature thermal conductivity.

As it has been mentioned above, we assume here that the contribution of N-processes can be neglected in comparison with other scattering mechanisms (U-processes and static defects) in the materials of interest. The phonon free path length related to the U-type phonon–phonon scattering ($l_{\mathrm{U}(i)}$) decreases with temperature and with the phonon frequency. Following the analysis of Slack [12], at high temperatures it is proportional to $\sim T^{-1}\omega^{-2}$. Moreover, the phonon path should be inversely proportional to the mean number of the phonons excited at the given temperature which is determined by the Bose function. Then one can expect for the whole temperature range:

$$\Lambda_{\mathrm{ph}} \approx \frac{l_{\mathrm{U}}(\omega)}{l_0} = A_{\mathrm{U}} \cdot (\mathrm{e}^{\bar{\theta}/b_{\mathrm{U}}T} - 1) \cdot \frac{\theta_i^2}{T^2} \cdot \frac{\omega_{i\max}^2}{\omega^2}, \qquad (19)$$

where A_{U} and b_{U} are dimensionless constants determined by the solid structure and properties. The constant b takes into account that not all phonons can participate in U-processes ($b_{\mathrm{U}} = 2$–8 in most of practical cases; below we use $b_{\mathrm{U}} = 4$ as the first guess). The expression for the thermal conductivity, limited by phonon–phonon scattering processes described by (19), can be presented as follows:

$$\kappa_{\mathrm{ph\,U}}(T) = \frac{\kappa_0 \cdot A_{\mathrm{U}} \cdot (\mathrm{e}^{\bar{\theta}/b_{\mathrm{U}}T} - 1)}{3N_{\mathrm{cell}}} \cdot \left(\frac{u_{\mathrm{AL}}}{u_0} \cdot D_1'(\theta_{\mathrm{AL}}/T) + \frac{2 \cdot u_{\mathrm{AT}}}{u_0} \cdot D_1'(\theta_{\mathrm{AT}}/T) \right). \qquad (20)$$

The coefficient A_{U} can be determined from the high temperature approximation of (20) using the relationship for the intrinsic thermal conductivity of a Debye type solid at high temperatures, which was first deduced by Leibfried and Schlömann [16] and then corrected by Julian [17] and by Slack [12]. It allows obtaining the following expression:

$$A_{\mathrm{U}} = 5.84 \cdot 10^{-23} \left(\frac{k_{\mathrm{B}}}{2\pi\hbar} \right)^3 \cdot \frac{\overline{M} \cdot N_{\mathrm{cell}}^{1/3} \cdot \bar{\theta}^2}{n_{\mathrm{at}}^{1/3} \cdot \kappa_0 \cdot \gamma_{\mathrm{G}}^2}, \qquad (21)$$

where $\overline{M}_{\mathrm{at}}$ is the mean mass number.

The relationships (19) and (21) are rough approximations that valid in the case where the contribution of N-processes is small. They can give rather satisfactory results within a group of the similar materials in many cases, but sometimes a fine fitting of the scattering coefficients is still needed. The U-processes parameter b_{U} remains free and should be chosen in every case to assure a better agreement at high temperatures.

6. Results of modelling

The calculation of the heat capacity, the thermal expansion coefficient, and the thermal conductivity of the materials of interest with the above formulae requires knowledge of their density, elastic moduli, Gruneisen parameter, crystal structure, lattice parameters, frequency limits of the phonon spectra branches, spectrum of the electronic excitations, and information about point defects and crystallite sizes. For the oxides considered in this article, the values of input parameters at standard temperature and pressure (STP) used in the calculations are presented in Table 1.

Table 1
Some parameters of the considered oxides at STP used as input

		UO_2	ThO_2	ZrO_2
Molecular mass	g mol^{-1}	270.03	264.04	123.22
Crystal structure		FCC fluorite type	FCC fluorite type	Monoclinic $P2_1/c$
Lattice parameter	10^{-9} m	0.5470	0.5597	0.5143 0.5194 0.5298 ($\beta = 99.22°$)
Theoretical density	kg m^{-3}	10956	10002	5860
Lattice volume	10^{-30} m^3	163.7	175.3	139.7
Young modulus	10^{11} Pa	2.33	2.61	2.10
Poisson's ratio	–	0.32	0.28	(0.33)
$\omega_{\mathrm{AL}}/\omega_{\mathrm{OL\,min}}/\omega_{\mathrm{OL\,max}}$	–	1.0/1.0/3.6	1.0/1.0/3.6	1.0/1.0/3.6
$\omega_{\mathrm{AT}}/\omega_{\mathrm{OT\,min}}/\omega_{\mathrm{OT\,max}}$	–	1.0/1.9/3.9	1.0/1.9/3.9	1.0/1.5/3.0
Grunëisen parameter	–	1.9	1.8	1.3

6.1. Urania

For benchmarking of the model, the UO_2 case has been analysed first. As input information we used the lattice parameter, the elastic constants and the frequency limits for the optical branches cited in [7]. The temperature dependence of the bulk elastic modulus was taken from [18], and the Grüneisen parameter of 1.9 was recommended in [19] as the best estimate value for UO_2. The localised electron excitation levels were taken from [20]: two levels at 1246 cm^{-1}, three at 1372 cm^{-1} and one at 1425.5 cm^{-1}.

Fig. 1(a)–(c) show, respectively, the calculated values of the isobaric specific heat, the isobaric CTE, and the thermal conductivity for UO_2 of theoretical density as a function of temperature in the region of 30–2000 K. The recommended and some experimental data from the literature [21–31] are also plotted there. From Fig. 1(a) it can be seen that the calculated isobaric specific heat is in a good agreement with the experimental data overall the considered temperature range. For the isobaric thermal expansion coefficient, this agreement is less good (Fig. 1(b)). The remarkable underestimation is observed at $T > 1700$ K, which can be an indication of a supplementary anharmonic or defect contribution that was not taken into account in the model. The difference in the region of 300–500 K could be explained by an error of the CTE extraction from the experimental data on the thermal strain. The UO_2 thermal conductivity is described by the model rather well in the range of 300–2000 K (Fig. 1(c)). Unfortunately, we did not find experimental data on the UO_2 thermal conductivity and CTE at lower temperatures (<300 K).

6.2. Thoria

The input elastic parameters for ThO_2 were selected from non-exhaustive published data on polycrystalline thorium dioxide [32,33]. The value $\gamma_G = 1.8$ was chosen for the Grunëisen parameter, taking into account a large dispersion (from 1.5 to 2.0) in its recommended values. We did not found in literature the characteristic optic frequencies of ThO_2, therefore the frequencies ratio's of UO_2 were used in these calculations (see Table 1). In contrast to UO_2 and to some other actinides, the localised electronic excitations are absent in ThO_2. The results of calculations and some available experimental results [21,22,33–40] are presented in

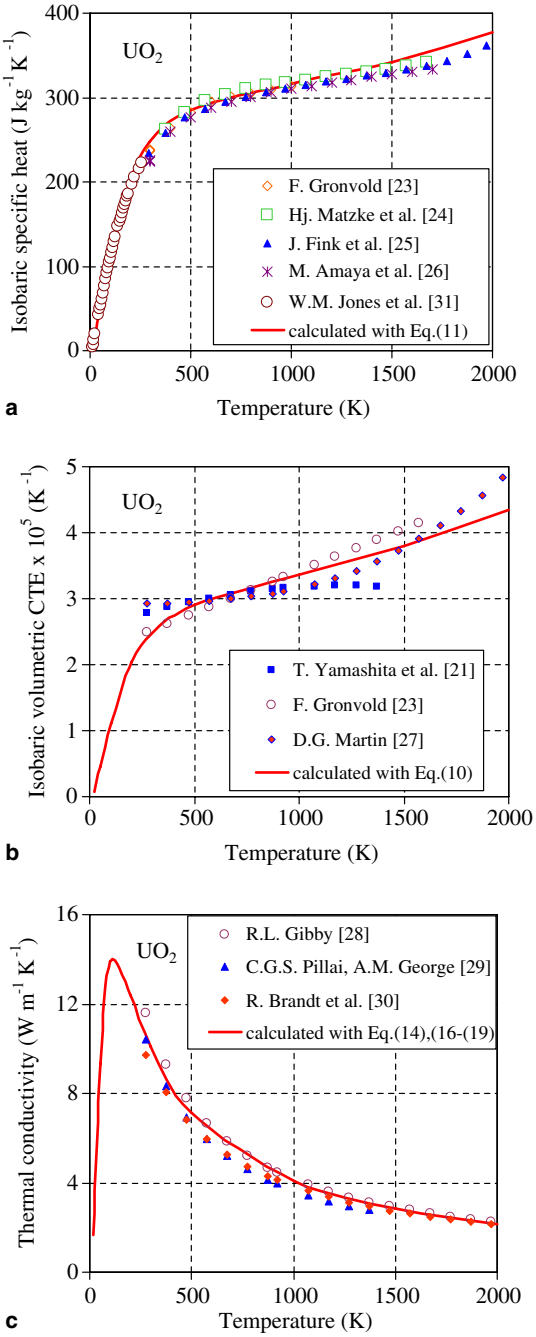

Fig. 1. Calculated with the parameters presented in Table 1 and experimental values of the isobaric specific heat (a), of the isobaric volumetric thermal expansion coefficient (b) and of the thermal conductivity (c) of UO_2 (all values are normalised to 100% TD).

Fig. 2. Similar to the case of UO_2, a good agreement between the calculated and recommended values has been obtained for the isobaric specific heat over the considered temperature region from 30 to

2000 K (Fig. 2(a)). The coefficient of thermal expansion of ThO_2 is also well described by the model – the calculated values are in the limits of the differences between the different experimental data up to 1600 K (Fig. 2(b)). The available experimental data on the thoria thermal conductivity also suffer from a remarkable dispersion. The calculated curve lies well within the region of the experimental points (Fig. 2(c)).

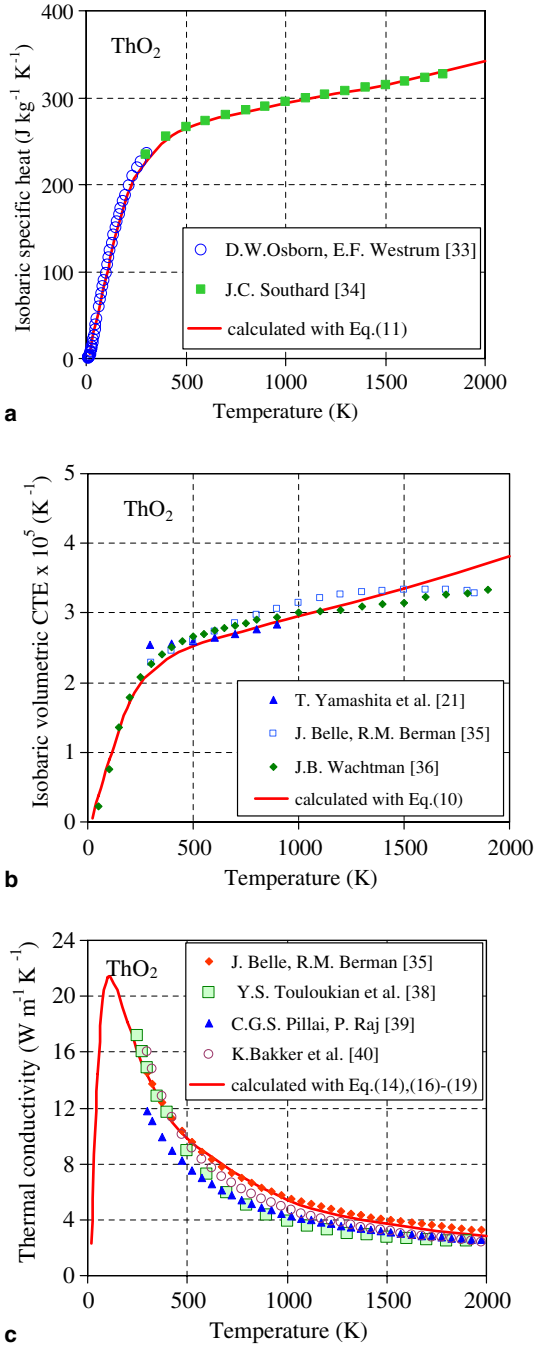

Fig. 2. Calculated with the parameters presented in Table 1 and experimental values of the isobaric specific heat (a), of the isobaric volumetric thermal expansion coefficient (b) and of the thermal conductivity (c) of ThO_2 (all values are normalised to 100% TD).

6.3. Zirconia

In spite of a lot of studies performed with zirconia, only a few publications exist that give the thermophysical and mechanical parameters of the pure monoclinic ZrO_2 over a large temperature range. In these calculations, the data presented in [22,37,38,41–53] and the isotropic model of ZrO_2 crystal with averaged parameters were used. The same optic frequency ratios were used as above but the gap between the acoustic and optic branches was reduced taking into account a lower M/O mass ratio in ZrO_2 compared to UO_2. The input parameters are given in Table 1. From Fig. 3(a) one can see that the isobaric specific heat is rather satisfactory described by the model up to the temperatures close to the temperature range where pure zirconia exhibits a monoclinic–tetragonal structural phase transformation (1440–1470 K [42,43]). The available data on the thermal expansion show a large dispersion between the values and in the temperature dependence [37,41,47,48,50]. The calculated CTE line passes just between them (Fig. 3(b)). It is rather close to the results obtained by Fehrenbacher and Jacobson [41]. The more consistent experimental data on the thermal conductivity of the pure monoclinic ZrO_2 were published in [43,49,53]. The detailed analysis of the ZrO_2 and YSZ thermal conductivity has recently been performed by Degueldre et al. [44], who mentioned a large uncertainty in the calculations of the coefficient (21) related to U-processes. In the current calculation, this parameter was fitted to the experimental results obtained with a quasi-monocrystal of the monoclinic ZrO_2 [43] at high temperatures, and the scattering coefficient of static defects was found using the data at room temperature. The thermal conductivity calculated with the model in the whole temperature range is in satisfactory agreement with the experimental results up to about 1100 K (Fig. 3(c)). At higher temperatures, the experimental values of [43] are higher. The same tendency was also observed for the pure ZrO_2 polycrystalline sample of a low porosity (2.37%) [50]. Its thermal conductivity is a few times higher than the lowest thermal conductivity limit of ZrO_2 calculated

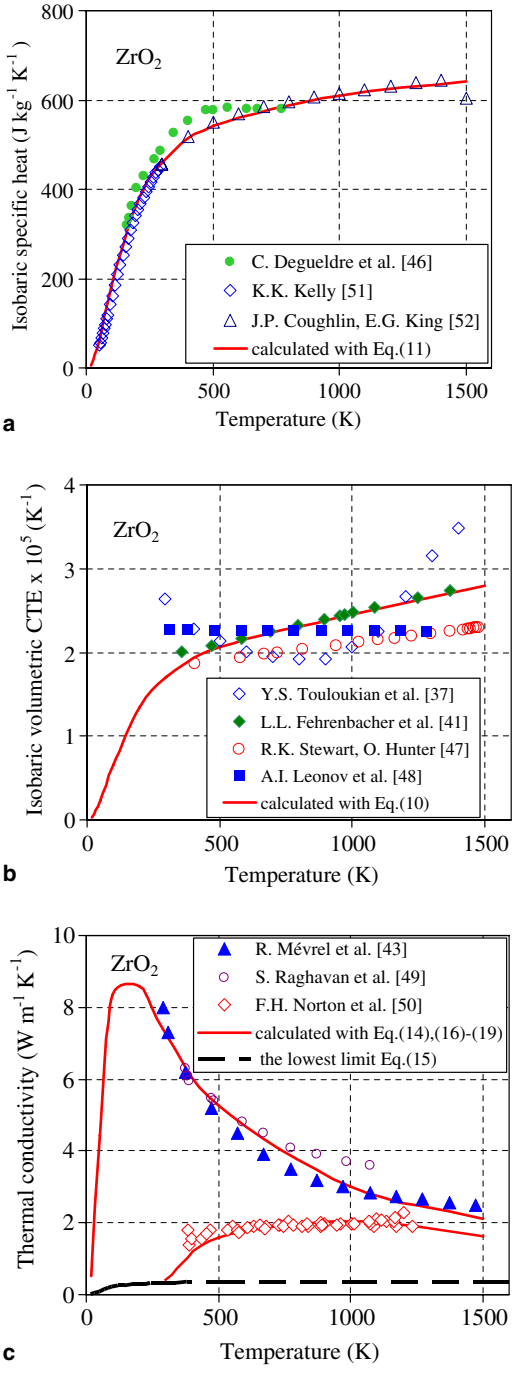

Fig. 3. Calculated with the parameters presented in Table 1 and experimental values of the isobaric specific heat (a), of the isobaric volumetric thermal expansion coefficient (b) and of the thermal conductivity (c) of ZrO_2 (all values are normalised to 100% TD).

with Eq. (15). This behaviour could be explained by a supplementary contribution of non-phonon mechanisms, e.g. by photons. A more detailed analysis is needed to explain this effect.

7. Conclusions

In the framework of studies of the thermal and mechanical properties of oxide IMF, a simplified model was proposed and some expressions were deduced for the calculation of heat capacity, thermal expansion, and thermal conductivity of dioxides of interest, aiming at the implementing in mechanistic fuel performance codes. The model is based on a simplified phonon spectrum, a quasi-harmonic approximation for the lattice vibrations, and the Klemens model for thermal conductivity. The developed model was successfully tested using the available data for the isobaric specific heat, the isobaric coefficient of thermal expansion, and the thermal conductivity of UO_2. Then the model was applied for the calculation of the same properties of ThO_2 and ZrO_2. A good agreement has been obtained over a large temperature region for all considered parameters of ThO_2 and for the isobaric specific heat and CTE of ZrO_2. Some difficulties still exist in the modelling of the thermal conductivity of zirconia.

The developed methodology completed by the similarity principle can be applied for prediction of thermal properties of other forms of nuclear fuels and materials for which the data are still unavailable or incomplete.

Acknowledgement

This work was supported by funds of the MYRRHA project of SCK·CEN and by the FUTURE project of the EURATOM 5th Framework Programme.

References

[1] C.B. Basak, A.K. Sengupta, H.S. Kamath, J. Alloys Compd. 360 (2003) 210.
[2] K. Kurosaki, K. Yamada, M. Uno, Sh. Yamanaka, K. Yamamoto, T. Namekawa, J. Nucl. Mater. 294 (2001) 160.
[3] T. Arima, K. Fukuyo, K. Idemitsu, Y. Inagaki, J. Mol. Liquids 113 (2004) 67.
[4] C. Kittel, Thermal Physics, Wiley, New York, 1976.
[5] C. Kittel, Introduction to Solid State Physics, 2nd Ed., Wiley, New York, 1956.
[6] G.J. Hyland, J. Ralph, High Temp. High Press. 15 (1983) 191.
[7] G. Dolling, R.A. Cowley, A.D.B. Woods, Can. J. Phys. 43 (1965) 1397.

[8] V. Sobolev, J. Nucl. Mater. 344 (2005) 198.
[9] O.L. Anderson, Equation of State of Solids for Geophysics and Ceramic Science, Oxford University, NY, 1995.
[10] P.G. Klemmens, Theory of the thermal conductivity of solids, in: R.P. Tye (Ed.), Thermal Conductivity, Academic Press, NY, 1969, p. 1.
[11] S.E. Lemehov, V. Sobolev, P. Van Uffelen, J. Nucl. Mater. 320 (2003) 66.
[12] G.A. Slack, The Thermal Conductivity of Non-metallic Crystals, in: H. Ehrehrech, F. Scitz, D. Turnbull (Eds.), Solid State Physics, vol. 34, Academic Press, New York, 1979.
[13] H.B.G. Casimir, Physica (Utrecht) 5 (1938) 495.
[14] P.G. Klemmens, Thermal Conductivity and Lattice Vibrational Modes, in: H. Ehrehrech, F. Scitz, D. Turnbull (Eds.), Solid State Physics, vol. 7, Academic Press, New York, 1959.
[15] J.M. Ziman, Electrons and Phonons. The Theory of Transport Phenomena in Solids, Oxford Classics Series, Clarendon, Oxford, 2001.
[16] G. Leibfried, E. Schlölann, Nachr. Akad. Wiss. Göttingen, Math.-Physik. K1 2a (1954) 71.
[17] C.L. Julian, Phys. Rev. A 137 (1965) 128.
[18] J.B. Wachtman, M.L. Wheat, H.J. Anderson, J.L. Bates, J. Nucl. Mater. 16 (1965) 39.
[19] A.C. Momin, M.D. Karkhanavala, High Temp. Sci. 10 (1978) 45.
[20] J.C. Krupa, Z. Gajek, Eur. J. Solid State Inorg. Chem. 28 (1991) 143.
[21] T. Yamashita, N. Nitani, T. Tsuji, H. Inagaki, J. Nucl. Mater. 245 (1997) 72.
[22] Specific Heat-Nonmetalic SolidsY.S. Touloukian, E.H. Buyco (Eds.), The TRPC Data Series, vol. 5, Plenum, NY, Washington, 1970.
[23] F. Grønvold, N.J. Kvetseth, J. Chem. Thermodyn. 2 (1970) 665.
[24] Hj. Matzke, P.G. Lucuta, R.A. Verrall, J. Henderson, J. Nucl. Mater. 247 (1997) 121.
[25] J. Fink, M.G. Chasanov, L. Leibowitz, J. Nucl. Mater. 102 (1981) 17.
[26] M. Amaya, K. Une, K. Minato, J. Nucl. Mater. 294 (2001) 1.
[27] D.G. Martin, J. Nucl. Mater. 152 (1988) 94.
[28] R.L. Gibby, J. Nucl. Mater. 38 (1971) 163.
[29] C.G.S. Pillai, A.M. George, J. Nucl. Mater. 200 (1993) 78.
[30] R. Brandt, G. Neuer, Non-Equilib. Thermodyn. 1 (1976) 3.
[31] W.M. Jones, J. Gordon, E.A. Long, J. Chem. Phys. 20 (1952) 695.
[32] M. Hoch, J. Nucl. Mater. 130 (1985) 94.
[33] D.W. Osborn, E.F. Westrum Jr., J. Chem. Phys. 21 (1953) 1884.
[34] J.C. Southard, J. Am. Chem. Soc. 63 (1941) 3142.
[35] J. Belle, R.M. Berman, Thorium dioxide: properties and nuclear applications, Naval Reactors Office, USDOE, DOE/NE-0060, 1984.
[36] J.B. Wachman, T.G. Scudert, G.W.J. Cleek, J. Am. Ceram. Soc. 45 (1962) 319.
[37] Thermal Expansion – Nonmetallic SolidsY.S. Touloukian, R.K. Kirby, R.E. Taylor, T.Y.R. Lee (Eds.), The TRPC Data Series, vol. 13, Plenum, NY, Washington, 1977.
[38] Thermal Conductivity – Nonmetalic SolidsY.S. Touloukian, R.W. Powel, C.Y. Ho, P.G. Klemens (Eds.), The TRPC Data Series, vol. 2, Plenum, NY, Washington, 1970.
[39] C.G.S. Pillai, P. Raj, J. Nucl. Mater. 277 (2000) 116.
[40] K. Bakker, E.H.P. Cordfunke, R.J.M. Konings, R.P.C. Schram, J. Nucl. Mater. 250 (1997) 1.
[41] L.L. Fehrenbacher, L.A. Jacobson, J. Am. Ceram. Soc. 88 (3) (1965) 157.
[42] J.W. Adams, H.H. Nakamura, R.P. Ingel, R.W. Rice, J. Am. Ceram. Soc. 68 (1985) C228.
[43] R. Mévrel, J.-C. Laizet, A. Azzopardi, B. Leclercq, M. Poulain, O. Lavigne, D. Demange, J. Eur. Ceram Soc. 24 (2004) 3081.
[44] C. Degueldre, T. Arima, Y.W. Lee, J. Nucl. Mater 319 (2003) 6.
[45] A. Mondal, S. Ram, Chem. Phys. Lett. 382 (2003) 297.
[46] C. Degueldre, P. Tissot, H. Lartigue, M. Pouchon, Thermochim. Acta 403 (2003) 267.
[47] R.K. Stewart, O. Hunter, J. Am. Ceram. Soc. 53 (1970) 421.
[48] A.I. Leonov, A.B. Andreeva, E.K. Keller, Izv. Akad. Nauk SSSR, Ser. Neorg. Mater. 2 (1) (1966) 137, English trans.: Inorg. Mater. (USSR) 2 (1966) 115.
[49] S. Raghavan, H. Wang, R.B. Dinwiddie, W.D. Porter, M.J. Mayo, Scri. Mater. 39 (1998) 1119.
[50] F.H. Norton, W.D. Kingery, D.M. Fellows, M. Adams, M.C. McQuarrie, R.L. Coble, USAEC Rept. NYO-596, 1950, p. 1.
[51] K.K. Kelly, Ing. Eng. Chem. 36 (1944) 377.
[52] J.P. Coughlin, E.G. King, J. Am. Chem. Soc. 72 (1950) 2262.
[53] C. Ronchi, J.P. Ottaviani, C. Degueldre, R. Calabrese, J. Nucl. Mater. 320 (2003) 54.